Received: 12 January 2024 | Revised: 16 August 2024 | Accepted: 5 September 2024

DOI: 10.1002/psp4.13245

ARTICLE

Physiology-based pharmacokinetic model with relative transcriptomics to evaluate tissue distribution and receptor occupancy of anifrolumab

Pradeep Sharma[1] | **David W. Boulton**[2] | **Lynn N. Bertagnolli**[2] | **Weifeng Tang**[2]

[1]Clinical Pharmacology and Quantitative Pharmacology, Clinical Pharmacology and Safety Sciences, R&D, AstraZeneca, Cambridge, UK

[2]Clinical Pharmacology and Quantitative Pharmacology, Clinical Pharmacology and Safety Sciences, R&D, AstraZeneca, Gaithersburg, Maryland, USA

Correspondence
Pradeep Sharma, AstraZeneca, Biomedical Campus, 1 Francis Crick Ave, Trumpington, Cambridge CB2 0AA, UK.
Email: pradeep.sharma@astrazeneca.com

Abstract

Type I interferons contribute to the pathogenesis of several autoimmune disorders, including systemic lupus erythematosus (SLE), systemic sclerosis, cutaneous lupus erythematosus, and myositis. Anifrolumab is a monoclonal antibody that binds to subunit 1 of the type I interferon receptor (IFNAR1). Results of phase IIb and phase III trials led to the approval of intravenous anifrolumab 300 mg every 4 weeks (Q4W) alongside standard therapy in patients with moderate-to-severe SLE. Here, we built a population physiology-based pharmacokinetic (PBPK) model of anifrolumab by utilizing the physiochemical properties of anifrolumab, binding kinetics to the Fc gamma neonatal receptor, and target-mediated drug disposition properties. A novel relative transcriptomics approach was employed to determine IFNAR1 expression in tissues (blood, skin, gastrointestinal tract, lungs, and muscle) using mRNA abundances from bioinformatic databases. The IFNAR1 expression and PBPK model were validated by testing their ability to predict clinical pharmacokinetics over a large dose range from different clinical scenarios after subcutaneous and intravenous anifrolumab dosing. The validated PBPK model predicted high unbound local concentrations of anifrolumab in blood, skin, gastrointestinal tract, lungs, and muscle, which exceeded its IFNAR1 dissociation equilibrium constant values. The model also predicted high IFNAR1 occupancy with subcutaneous and intravenous anifrolumab dosing. The model predicted more sustained IFNAR1 occupancy ≥90% with subcutaneous anifrolumab 120 mg once-weekly dosing vs. intravenous 300 mg Q4W dosing. The results informed the dosing of phase III studies of anifrolumab in new indications and present a novel approach to PBPK modeling coupled with relative transcriptomics in simulating pharmacokinetics of therapeutic monoclonal antibodies.

Study Highlights

WHAT IS THE CURRENT KNOWLEDGE ON THE TOPIC?

Previous studies have validated anifrolumab 300 mg intravenous (IV) every 4 weeks (Q4W) as the optimal dose for patients with SLE.

WHAT QUESTION DID THIS STUDY ADDRESS?

Can a population physiology-based pharmacokinetic (PBPK) model be coupled with a relative transcriptomics approach to predict local anifrolumab tissue concentrations and receptor occupancy, to guide dose selection for phase III anifrolumab studies in new indications?

WHAT DOES THIS STUDY ADD TO OUR KNOWLEDGE?

Anifrolumab 300 mg IV Q4W offers high local anifrolumab concentrations in target tissues and high receptor occupancy. Anifrolumab 120 mg administered subcutaneously every week is equivalent to 300 mg IV Q4W in achieving high local anifrolumab concentrations and high receptor occupancy; SC has lower variability in the unbound anifrolumab concentration across the dosing interval than IV.

HOW MIGHT THIS CHANGE DRUG DISCOVERY, DEVELOPMENT, AND/OR THERAPEUTICS?

We provide a novel modeling approach to target expression optimization and application in clinical development. The anifrolumab PBPK model may inform dosing of phase III anifrolumab trials for new indications.

INTRODUCTION

Type I interferons (IFNs) play an important role in the pathogenesis of several autoimmune disorders including systemic lupus erythematous (SLE), systemic sclerosis (SSc), and myositis.[1–4] There is strong evidence of elevated type I IFN signaling and gene signature (IFNGS) expression in these autoimmune diseases,[1–5] and type I IFN inhibition is an established treatment modality for patients with SLE.[6,7] Currently, there is an unmet need for additional disease-modifying therapies capable of halting or reversing the immune dysregulation in SSc and myositis.[2,8]

Anifrolumab (SAPHNELO® AstraZeneca, Södertälje, Sweden) is a fully human IgG1κ monoclonal antibody (mAb) that binds with high specificity and affinity to the type I IFN-α receptor (IFNAR1) subunit 1, leading to IFNAR1 internalization and inhibition of downstream IFNAR1-mediated signaling.[6] IFNAR1-blockade with anifrolumab inhibits IFN-responsive gene expression and downstream inflammatory and immunological processes that contribute to autoimmune disease pathologies.[5]

Intravenous (IV) anifrolumab is approved for patients with moderate-to-severe SLE receiving standard therapy, based on the results of three randomized, placebo-controlled trials.[6,9–11] Pharmacokinetic, efficacy, and safety data in patients with SLE from the phase IIb MUSE trial supported the optimal anifrolumab dosage of 300 mg every 4 weeks (Q4W) for the phase III TULIP trials.[9,12] In TULIP-1 and TULIP-2, anifrolumab IV 300 mg alongside standard therapy was associated with clinically meaningful improvements in disease activity.[6,10,11] A population-based pharmacokinetic model based on data from five clinical trials of anifrolumab IV Q4W exhibited nonlinear pharmacokinetics, time-varying linear clearance, and sustained concentrations supporting this dosing in patients with SLE.[13] Studies investigating subcutaneous (SC) anifrolumab administration are ongoing.[14–17]

Pharmacokinetics, safety, and tolerability of IV and SC anifrolumab were compared in a phase I randomized, placebo-controlled trial in healthy adults.[18] Anifrolumab 300 mg SC exposure was 87% of IV administration, and SC dosing was well tolerated.[18] Emerging evidence in patients with SLE indicates that patients would like both IV and SC administration options, further supporting research into SC administration.[19,20]

Physiology-based pharmacokinetic (PBPK) modeling offers a comprehensive understanding of how drug compounds distribute, metabolize, and interact within the human body and may support dose selection and trial design of studies for new indications.[21] Previous whole-body human PBPK modeling of intravenous IFN-α describing pharmacokinetics and subsequent IFN-α–IFNAR occupancy in the liver provided a framework for future model-based study design.[22] Here, we present population PBPK modeling of IV and SC anifrolumab to compare routes of administration and support dose selection and design of anifrolumab phase III studies for new indications, including lupus nephritis, cutaneous lupus erythematosus,

myositis, and SSc.[14–16,23] We use a novel relative transcriptomics approach for predicting IFNAR1 expression in blood, skin, lung, gastrointestinal tract, and muscle tissues.

METHODS

The PBPK modeling strategy was informed by three clinical trials of healthy populations and/or patients with SSc or SLE ($n = 49$).[18,24,25] Trial designs, populations, and anifrolumab dosages are summarized in Table S1 (Appendix S1: Section 1.0).[18,24,25]

The Simcyp population-based simulator (Certara UK Ltd., Sheffield, UK; Version 21)[26] was used for anifrolumab PBPK modeling, using default Simcyp parameter values to create a virtual healthy volunteer population (demographic, anatomical, and physiological parameters, including organ volumes and respective blood flows). Mean and distribution of demographic covariates (e.g., age, sex, body weight, body surface area, organ weight, and tissue composition) were generated using a correlated Monte Carlo approach under predefined study designs within Simcyp. The construction and validation of the Simcyp Biologics module were previously published.[27,28]

PBPK model structure

A whole body, fully mechanistic PBPK model was utilized to predict anifrolumab distribution after IV or SC administration by incorporating passive diffusion, convective transport, and transcytosis through vascular epithelial cells by Fc gamma neonatal receptor (FcRn; Appendix S1: Section 1.1). The full PBPK distribution model employed time-based differential equations to simulate anifrolumab concentrations in various organs: blood, adipose tissue, bone, brain, gut, heart, kidney, liver, lung, muscle, pancreas, skin, and spleen.[29] Elimination was modeled to incorporate linear clearance due to non-specific catabolic pathways, and specific clearance resulting from anifrolumab–IFNAR1 binding followed by internalization and subsequent lysosomal degradation (Appendix S1: Section 1.1).

PBPK modeling strategy

The anifrolumab PBPK modeling strategy was divided into construction, validation, and application (Figure 1). The following sections describe the methodologies within each step.

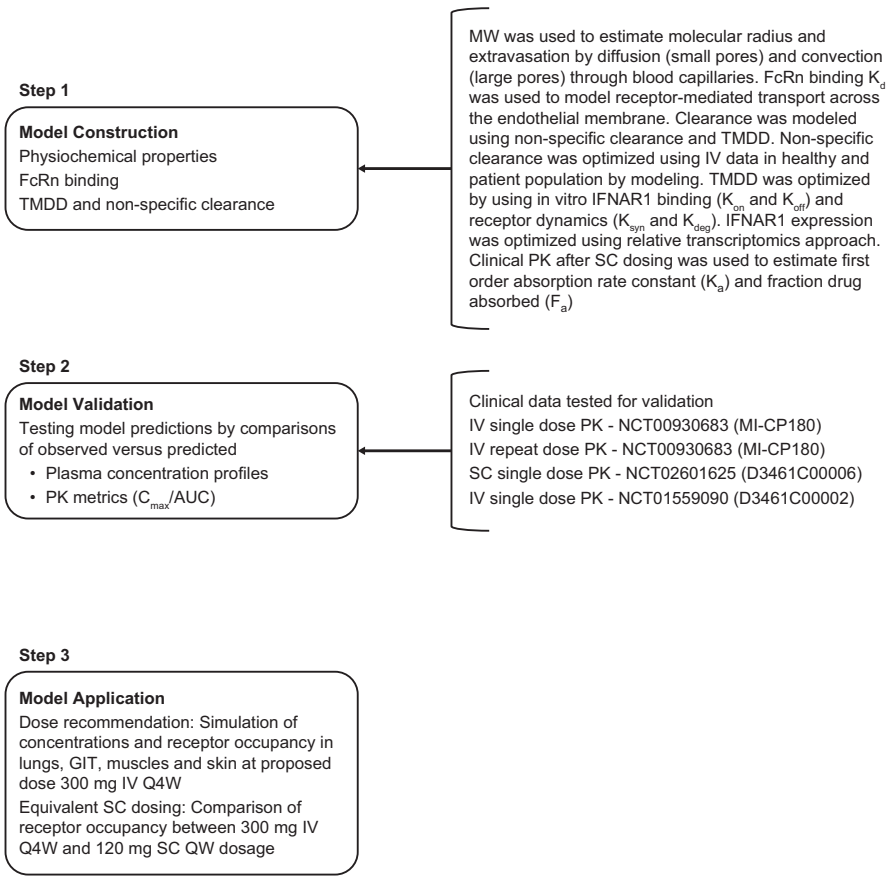

FIGURE 1 Schematic diagram to show PBPK modeling strategy. AUC, area under the serum concentration–time curve; C_{max}, maximum observed concentration in serum; F_a, fraction of drug absorbed; FcRn, Fc gamma neonatal receptor; GIT, gastrointestinal tract; IFNAR1, type I interferon receptor; IV, intravenous; K_a, first-order absorption rate constant; K_d, equilibrium dissociation constant; K_{deg}, receptor degradation rate constant; K_{off}, dissociation constant; K_{on}, association constant; K_{syn}, receptor synthesis rate constant; MW, molecule weight; PK, pharmacokinetics; Q4W, every 4 weeks; QW, once a week; SC, subcutaneous; TMDD, target-mediated drug disposition.

Model construction

The model development process used pharmacokinetics data from two phase I studies: anifrolumab 3 mg IV single dose (SD) data of four patients with SSc (NCT00930683)[24]; anifrolumab 300 mg IV and 300 mg SC data of 12 healthy volunteers (NCT02601625)[18] (Appendix S1: Section 1.0, Table S1). The anifrolumab PBPK model was developed through the "middle out" approach using the physiochemical properties of anifrolumab, FcRn binding, and TMDD properties (Appendix S1: Section 1.1, Table S2).

Molecular weight is an important input parameter in determining protein distribution[30] and was used to estimate molecular radius and extravasation by diffusion (small pores) and convection (large pores) through blood capillaries. The Simcyp platform PBPK model is optimized for endogenous IgG.[28] This in-built structural PBPK model was used with most parameters fixed based on the behavior of endogenous IgG. Anifrolumab in vitro values of FcRn K_d and clinical data were used to parameterize the TMDD aspects of the model and predict the compound pharmacokinetics in a population. Population pharmacokinetics modeling of anifrolumab showed that non-specific first-order catabolic clearance by the reticuloendothelial system (CL_{RES}) was 31% lower in IFNGS-low vs. IFNGS-high patients.[12] Patients with SLE with high IFNGS presented faster clearance of the first-order elimination pathway than those with low IFNGS, likely due to increased proteolytic catabolism owing to severe inflammation. Therefore, non-specific CL_{cat} was optimized by sensitivity analyses to match the observed clinical anifrolumab pharmacokinetics (Appendix S1: Sections 2.1–2.2, Tables S3–S6 and Figures S1–S4). In vitro binding parameters that encompassed the association and dissociation rate constants, coupled with receptor dynamics involving synthesis rate and degradation kinetics constant, were employed to enhance TMDD model precision.

IFNAR1 receptor abundance in tissues was extrapolated using a relative transcriptomics approach, which has been successfully applied to quantify the expression of drug-metabolizing enzymes and transporters to model the pharmacokinetics of small-molecule drugs.[31] In this approach, tissue-specific mRNA expression is used as a surrogate for protein abundance and activity, which is integrated into PBPK models. IFNAR1 abundance in the liver was previously reported.[22] IFNAR1 abundance in other tissues was extrapolated from liver abundance using the following formula:

$$T_{\text{IFNAR1}} = \frac{\text{nTPM}_{\text{T}}}{\text{nTPM}_{\text{L}}} \times L_{\text{IFNAR1}}$$

where T_{IFNAR1} is the IFNAR1 expression on tissue determined using relative transcriptomics. The IFNAR1 liver concentration (L_{IFNAR1}) was 0.242 nM based on work by Kalra[22] (see Appendix S1: Section 2.4 for methodological details). The mRNA transcript data, normalized IFNAR1 expression in tissue (nTPM_{T}), and normalized IFNAR1 expression in the liver (nTPM_{L}) were accessed online from the Human Protein Atlas transcriptomics database[32,33] on April 12, 2022 (Appendix S1: Section 2.3, Table S7 and Figure S5). Currently, there is a lack of quantitative data on the impact of autoimmune disease (e.g., SLE, SSc) pathophysiology on IFNAR1 abundance. However, in vitro and preclinical reports have shown that IFNAR1 expression is downregulated in cirrhotic liver tissues[34] or significantly upregulated in human peripheral blood T cells from patients with colorectal cancer.[35] Ultraviolet treatment has been shown to trigger ubiquitination and downregulation of IFNAR1 expression roughly twofold in human and mouse keratinocytes and skin tissues, alleviating psoriatic inflammation,[36] while free soluble IFNAR1 receptors were upregulated up to 10–25-fold in circulation in patients with various adenocarcinomas.[37] Due to uncertainty about the impact of autoimmune disease pathophysiology on IFNAR1 abundance, sensitivity analysis to assess the impact of optimized IFNAR1 abundance on receptor occupancy and local tissue concentrations was performed by increasing or decreasing IFNAR1 tissue abundance in steps of 1-, 2- and 5-fold after 300 mg IV dosing in patients with SSc and SLE.

The R_{max} in tissues was kept dynamic in the model and used to calculate the synthesis rate constant (K_{syn}) using the following formula[38] (Appendix S1: Section 2.4, Table S8):

$$R_{\text{max}} = \frac{K_{\text{syn}}}{K_{\text{deg}}}$$

The fraction of drug absorbed (F_a) and first-order absorption rate constant (K_a) were optimized by a sensitivity analysis to match the observed clinical anifrolumab pharmacokinetics after 300 mg single SC dosing from the phase I healthy volunteer trial (Appendix S1: Section 2.5, Figures S6–S8 and Table S9). The optimized values of F_a and K_a (0.80 and 0.014 1/h) are similar to those estimated using internal unpublished population pharmacokinetics modeling analysis (0.82 and 0.011 1/h, respectively).

Model validation

Model validation utilized clinical scenarios including 0.1, 0.3, 1, 10, 20 mg/kg IV SD, or 5 mg/kg IV every week (QW) in 22 patients with SSc (phase I trial; NCT00930683),[24] 600 mg SC SD in six healthy volunteers (phase I trial; NCT02601625),[18] and 300 mg IV SD in five patients with SLE (phase II trial; NCT01559090)[25] (Appendix S1: Sections 1.0 and 3.0, Table S1). The comparison between

anifrolumab simulated and observed serum concentration profiles, as well as pharmacokinetic parameters (C_{max} and AUC), were used to determine the PBPK model credibility.

Metrics were applied to observed and predicted pharmacokinetic parameters to assess the PBPK model's predictive power. Geometric mean fold error (GMFE), an indicator of prediction bias, was used to compare observed and predicted pharmacokinetic values using the following formula:

$$\mathrm{GMFE} = 10^{\frac{1}{n}\sum \log \frac{\mathrm{Pred}_i}{\mathrm{Obs}_i}}$$

GMFE values range from 0 to infinity. Model predictions were considered satisfactory if GMFE ≥0.8–≤1.25, acceptable if GMFE ≥0.5–<0.8 or GMFE >1.25–≤2, and poor if GMFE <0.5 or GMFE >2.

Absolute average fold error (AAFE) measures the spread of the predictions by converting negative log fold errors to positive values before averaging using the following formula:

$$\mathrm{AAFE} = 10^{\frac{1}{n}\sum \left|\log \frac{\mathrm{Pred}_i}{\mathrm{Obs}_i}\right|}$$

AAFE values range from 1 to infinity. A prediction was considered satisfactory if AAFE ≤1.25, acceptable if AAFE >1.25–≤2, and poor if AAFE >2.

Percent prediction error (%PPE) and mean absolute prediction error (MAPE) were calculated as follows to determine model accuracy and precision, respectively:

$$\mathrm{PPE}(\%) = \left(\frac{\mathrm{Pred}_i - \mathrm{Obs}_i}{\mathrm{Obs}_i}\right) \times 100$$

$$\mathrm{MAPE}(\%) = \frac{1}{n}\sum_{i=1}^{n} |\mathrm{PPE}i|$$

Lower %PPE and MAPE values indicated better prediction.

Model application

The validated model was applied to predict local anifrolumab concentrations and receptor occupancy in skin, lung, gastrointestinal tract (GIT), and muscles using 300 mg Q4W IV dosing to support new indications. In addition, anifrolumab 300 mg IV Q4W was compared with 120 mg SC QW in 10 patients with SSc to assess local concentrations in target tissues and receptor occupancy.

Clinical trial simulation designs

In the simulations for model development and validation, age, weight, height, and sex were matched with the demographic information reported in the corresponding clinical studies.[18,24,25] Dosing regimens were consistent with the actual trial design (Appendix S1: Sections 1.0 and 4.0, Tables S1 and S10).

Ten virtual trials were simulated for each of the three trials in Table S1 (Appendix S1: Section 1.0) to predict population variability, such that each simulated trial contained the same number of subjects as the actual study. Three virtual populations were generated from the Simcyp population library, each adapted to include IFNAR1 expression (Appendix S1: Section 2.4, Table S8) and optimized CL_{cat} (Appendix S1: Sections 2.1–2.2). The different population models (healthy, patient, and Japanese patient populations) used to simulate clinical trials are listed in Appendix S1: Section 4.0 (Table S11). Randomization in the selection of virtual individuals was set in the Simcyp Simulation Toolbox, by keeping default settings to "Fixed Seed Random Distribution" and keeping the seed variable for fixed seed to "1." Table S10 (Appendix S1: Section 4.0) shows the simulation designs used in model development, validation, and application.

RESULTS

Model validation

The anifrolumab PBPK model predicted pharmacokinetic parameters (C_{max} and AUC) over a dose range of 0.1–20 mg/kg with single or repeat IV dosing in patients with SSc, single SC dosing in healthy volunteers, and single IV dosing in patients with SLE. The model also compared predicted C_{max} and AUC values with observed pharmacokinetic parameters from clinical trials. The model-predicted and observed geometric mean C_{max} and AUC values are shown in Table 1. For example, in patients with SSc administered anifrolumab 5 mg/kg IV QW, predicted C_{max} was 202 μg/mL, and observed C_{max} was 133 μg/mL. In patients with SLE administered anifrolumab 300 mg IV SD, predicted C_{max} was 103 μg/mL and observed C_{max} was 75.1 μg/mL. In healthy volunteers administered anifrolumab 600 mg SC SD, predicted C_{max} was 60.8 μg/mL and observed C_{max} was 60.5 μg/mL.

%PPE for C_{max} and AUC for each dose level ranged from −6% to 52% for C_{max} and −14% to 21% for AUC (Table 1). High %PPE for C_{max} may be related to the sensitivity of point estimates to sampling times and the sparsity of sampling in the clinical studies (5 mg/kg weekly IV QW). The bias and precision in the prediction ability of the anifrolumab PBPK model were also determined by calculating the GMFE, AAFE, and MAPE for eight different clinical scenarios (0.1 mg/kg IV SD, 0.3 mg/kg IV SD, 1 mg/kg IV SD, 10 mg/kg IV SD, 20 mg/kg IV SD, 5 mg/kg

TABLE 1 Comparison of predicted vs. observed PK parameters (C_{max} and AUC) of anifrolumab.

Clinical study	Anifrolumab dose, schedule, and route of administration	Predicted PK parameters		Observed PK parameters			Percent prediction error (%PPE)	
		C_{max} (μg/mL) geometric mean (%gCV)	AUC (μg.day/mL) geometric mean (%gCV)	Number of participants	C_{max} (μg/mL) geometric mean (%gCV)	AUC (μg.day/mL) geometric mean (%gCV)	C_{max}	AUC
Phase I SSc patient trial (NCT00930683)[24]	0.1 mg/kg, IV, SD	2.14 (15)	2.39 (25)	1	1.97 (NA)	2.45 (NA)	8.6	2.4
	0.3 mg/kg, IV, SD	6.18 (11)	13.2 (20)	4	6.58 (21)	11.6 (43)	−6.1	−14
	1 mg/kg, IV, SD	22.5 (24)	88.9 (22)	4	23.2 (10)	101 (14)	−3	12
	10 mg/kg, IV, SD	233 (23)	2013 (24)	4	209 (21)	2534 (29)	11.5	20.6
	20 mg/kg, IV, SD	468 (12)	4754 (21)	4	388 (20)	4515 (45)	20.6	−5.3
	5 mg/kg weekly, IV, QW[a]	202 (14)	949 (18)	5	133 (19)	838 (19)	51.9	−13.2
Phase II SLE patient trial (NCT01559090)[18]	300 mg, IV, SD	103 (14)	815 (18)	5	75.1 (13)	750 (34)	37.2	−8.7
Phase I healthy volunteer trial (NCT02601625)[25]	600 mg, SC, SD	60.8 (25)	1830 (33)	6	60.5 (39)	1949 (51)	0.5	6.1

Abbreviations: %PPE, percent prediction error; AUC, area under the serum concentration–time curve; CI, confidence interval; C_{max}, maximum observed concentration in serum; gCV, geometric coefficient of variation; IV, intravenous; NA, not applicable; PK, pharmacokinetics; QW, every week; SC, subcutaneous; SD, single dose; SLE, systemic lupus erythematosus; SSc, systemic sclerosis.

[a] $n = 3$ received repeat dosing and used to calculate $AUC_{0\text{-}7day}$ and C_{max} after 4th dose.

IV QW, 300 mg IV SD, 600 mg SC SD). Values for GMFE (C_{max}: 1.14, AUC: 0.99), AAFE (C_{max}: 1.16, AUC: 1.11), and MAPE (C_{max}: 17.4%, AUC: 10.3%), all fell within "satisfactory" or "acceptable" ranges, suggesting the model predicted observed values sufficiently.

Simulated serum concentration–time profiles overlaid on observed anifrolumab concentrations after IV or SC dosing over a large dose range were generally similar (Appendix S1: Section 5.0, Figures S9–S12).

Sensitivity analyses were used to predict the impact of changes in IFNAR1 abundance after anifrolumab 300 mg IV SD and the subsequent impact on mean anifrolumab serum concentration profile (simulations of $n = 100$ subjects). A significant impact on mean anifrolumab serum concentrations was observed when IFNAR1 abundance was increased or decreased by 2- to 5-fold (Appendix S1: Section 5.0, Figure S13).

To predict the impact of variations in IFNAR1 abundance in different tissues (lungs, GIT, muscles, and skin), a sensitivity analysis of IFNAR1 abundance variation on mean local anifrolumab concentration profile and mean IFNAR1 occupancy (simulations of $n = 100$ subjects) after 300 mg IV SD was conducted across these tissues. As in blood, IFNAR1 variation (increase or decrease by 2- to 5-fold) was predicted to significantly impact mean anifrolumab concentrations and IFNAR1 occupancy in the lungs, GIT, muscle, and skin (Appendix S1: Section 5.0, Figures S14 and S15).

Model application

We applied the validated PBPK model to predict unbound anifrolumab local concentrations in the lung, GIT, muscle, and skin with 300 mg IV Q4W in patients with SLE and SSc (Figure 2). The mean predicted concentrations of unbound anifrolumab after 300 mg IV Q4W were well above the anifrolumab affinity value ($K_d = 0.041$ µg/mL)

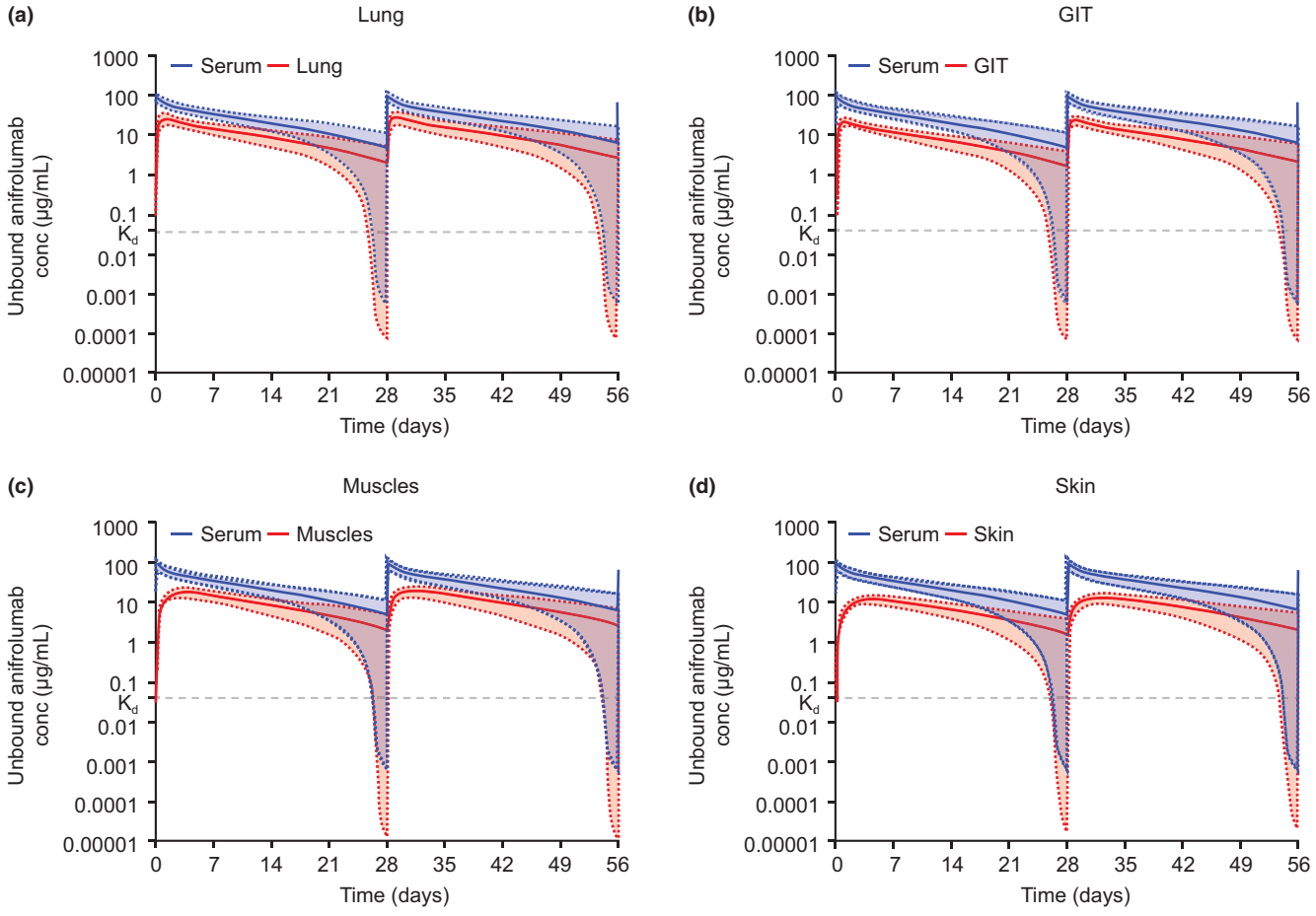

FIGURE 2 The mean concentration of unbound anifrolumab after 300 mg IV Q4W dosing in the SSc and SLE patient population in (a) lung, (b) GIT, (c) muscles, and (d) skin; the colored solid lines represent the mean predicted anifrolumab concentration; the colored dotted lines and shaded area represent the 5th and 95th percentiles of the simulation ($n = 100$); the dotted gray line is anifrolumab affinity ($K_d = 0.041$ µg/mL) for the IFNAR1 receptor. Conc, concentration; GIT, gastrointestinal tract; IFNAR1, type I interferon receptor; IV, intravenous; K_d, equilibrium dissociation constant; Q4W, every four weeks; SLE, systemic lupus erythematosus; SSc, systemic sclerosis.

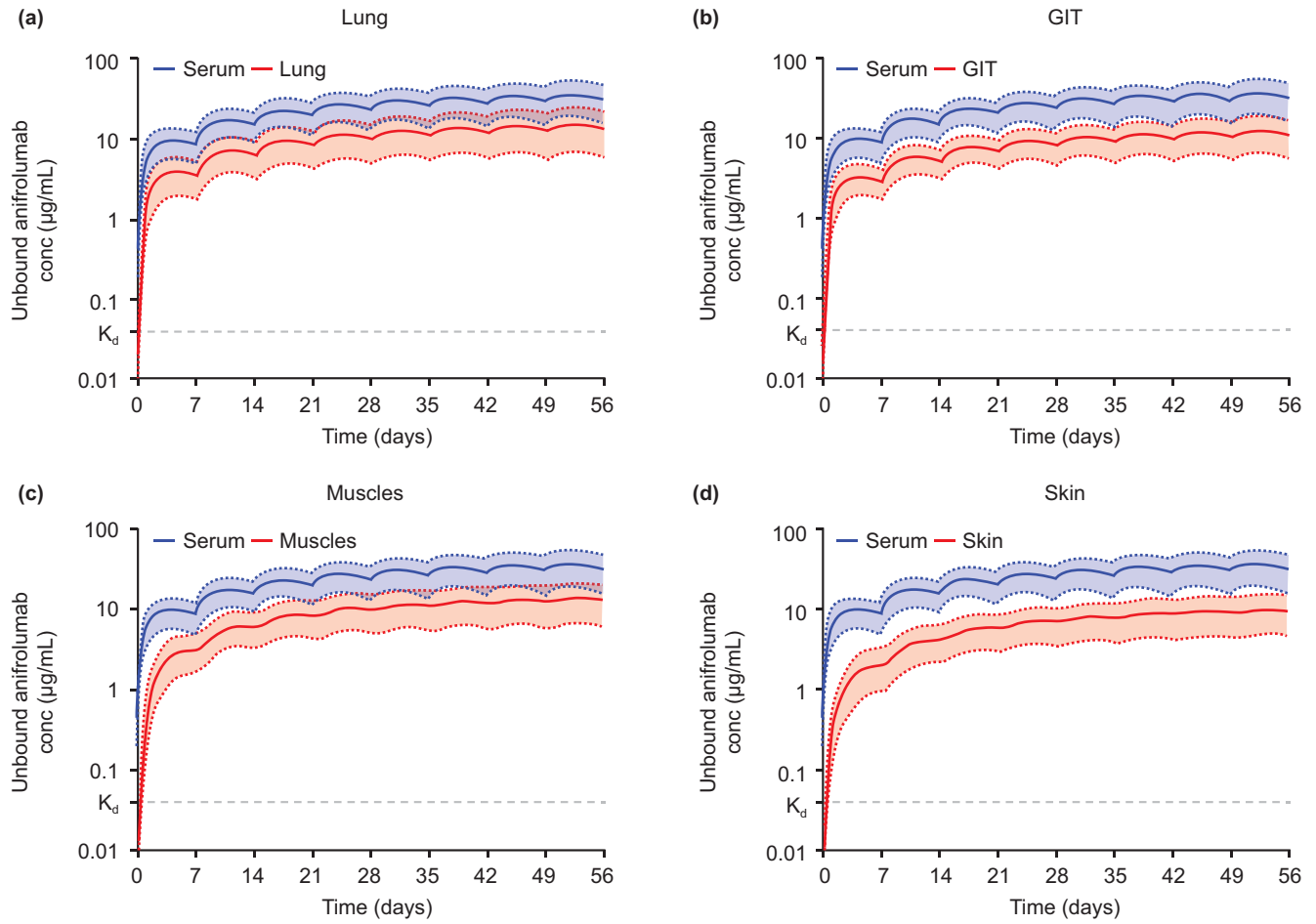

FIGURE 3 Mean concentration of unbound anifrolumab after 120 mg SC QW dosing in the SSc and SLE patient population in (a) lung, (b) GIT, (c) muscles, and (d) skin; the colored solid lines represent the mean predicted anifrolumab concentration; the colored dotted lines and shaded area represent the 5th and 95th percentiles of the simulation ($n = 100$); the dotted gray line is anifrolumab affinity ($K_d = 0.041$ µg/mL) for the IFNAR1 receptor. Conc, concentration; GIT, gastrointestinal tract; IFNAR1, type I interferon receptor; K_d, equilibrium dissociation constant; QW, once a week; SC, subcutaneous; SLE, systemic lupus erythematosus; SSc, systemic sclerosis.

in all assessed tissues, and anifrolumab concentrations gradually declined between doses.

To test the equivalence of 120 mg SC QW and 300 mg IV Q4W dosing, we applied the PBPK model to predict local unbound anifrolumab concentrations in the skin, lung, GIT, and muscle in patients with SLE and SSc with 120 mg SC QW (Figure 3). After 120 mg SC QW, predicted unbound anifrolumab concentrations were also above the K_d value for the IFNAR1 receptor, with frequent small fluctuations between weekly doses. To compare tissue pharmacokinetics vs. target concentrations, the simulated IFNAR1 receptor concentrations after 300 mg IV Q4W and 120 mg SC QW dosing in different target organs are included in Appendix S1: Section 6.0 (Figures S16 and S17).

Next, we compared the predicted unbound anifrolumab concentration in serum with 300 mg IV Q4W and 120 mg SC QW dosing in patients with SLE and SSc (Figure 4). Predicted unbound anifrolumab serum concentrations increased at an initially slower rate with SC compared with IV administration. However, SC administration resulted in more consistent concentration levels than IV administration, with frequent smaller fluctuations over time and lower variability assessed using 5th–95th confidence intervals.

Lastly, to assess the differences in local anifrolumab tissue concentration between IV and SC administration, we compared the predicted IFNAR1 receptor occupancy with 300 mg IV Q4W and 120 mg SC QW dosing in the lung, GIT, muscles, and skin in patients with SLE and SSc (Figure 5). With 300 mg IV Q4W dosing, ≥90% receptor occupancy was achieved within 3 hours and then fell below 90% after 25 days in all assessed tissues. With 120 mg SC QW dosing, ≥90% receptor occupancy was achieved between 1 and 3 days and was subsequently maintained consistently above 90% in all assessed tissues. With both anifrolumab IV and SC administration, receptor occupancy reached ≥90% faster in the lung and GIT than in skin and muscle.

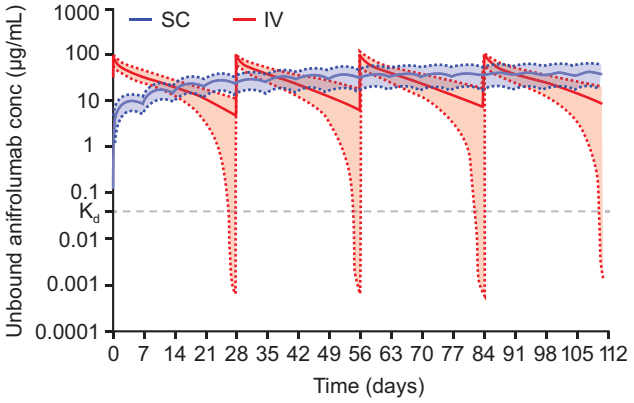

FIGURE 4 Comparison of mean unbound serum concentration of anifrolumab after 300 mg IV Q4W and 120 mg SC QW dosing in the SSc and SLE patient population; the colored solid lines represent the mean predicted anifrolumab concentration; the colored dotted lines and shaded area represent the 5th and 95th percentiles of the simulation ($n = 100$); the dotted gray line is anifrolumab affinity ($K_d = 0.041$ µg/mL) for the IFNAR1 receptor. Conc, concentration; IFNAR1, type I interferon receptor; IV, intravenous; K_d, equilibrium dissociation constant; Q4W, every 4 weeks; QW, once a week; SC, subcutaneous; SLE, systemic lupus erythematosus; SSc, systemic sclerosis.

DISCUSSION

Blocking IFNAR1 signaling with anifrolumab is a potential therapeutic option for IFN-mediated diseases, such as SSc, cutaneous lupus erythematosus, and myositis,[5] for which additional disease-modifying therapies are needed.[2,8,39] IFNAR1 distribution is widespread throughout the human body, encompassing organs, such as the lung, GIT, muscle, and skin, all of which can be clinically affected in patients with IFN-mediated diseases.[4,40,41] There is limited modeling data for anifrolumab–IFNAR1 physiological pharmacokinetics across different organ tissues as opposed to in serum. A further unmet need is to establish pharmacokinetic modeling for anifrolumab SC administration and evaluate the impact of IV and SC administration on anifrolumab-IFNAR1 pharmacokinetics. To address these unmet needs, we developed a whole body, fully mechanistic anifrolumab population PBPK model using a relative transcriptomics approach to predict IFNAR1 abundance in tissues and incorporating passive diffusion, convective transport, and transcytosis through vascular epithelial cells by FcRn. The model was validated over a wide anifrolumab dose range (0.1 mg/kg–20 mg/kg IV SD, 5 mg/kg IV QW, 300 mg IV SD, and 600 mg SC SD) and across multiple clinical scenarios and it reliably predicted anifrolumab pharmacokinetics in patients with SLE or SSc, and healthy volunteers.

Our validated PBPK model was applied to predict local anifrolumab concentrations and IFNAR1 occupancy in the skin, lung, GIT, and muscle with 300 mg IV Q4W (approved anifrolumab dosage in patients with SLE).[6] Unbound anifrolumab concentrations exceeded the K_d value for the IFNAR1 receptor with a ≥90% mean receptor occupancy in lungs, GIT, skin, and muscles for up to 28 days. In a separate study, higher anifrolumab concentrations (in serum) were associated with both the extent of IFNGS pharmacodynamic suppression and efficacy in patients with moderate-to-severe SLE.[42] Together, our findings support the potential for anifrolumab to bind IFNAR1 and suppress IFNAR1 signaling in the lungs, GIT, skin, and muscles in addition to in blood. Elevated IFNGS in tissues (including the skin and muscle) has been detected in patients with IFN–driven diseases such as SSc and myositis[43]; as such, local IFNAR1 inhibition in tissues could have a substantial clinical impact in patients with IFN-driven diseases.

Patient preference for SC vs. IV administration varies based on individual motivators and contextual factors, highlighting the importance of administration options.[20] To investigate 120 mg SC QW and 300 mg IV Q4W equivalence, we simulated concentration profiles and receptor occupancy in serum and target tissues with SC and IV dosing. While SC QW dosing showed a slower rate of receptor occupancy in serum initially compared with IV Q4W, SC administration achieved a constant high receptor occupancy at a steady state in the lung, GIT, muscles, and skin that fluctuated less than with IV. In all tissues assessed, receptor occupancy at a steady state decreased below 90% at Day 23 with IV Q4W dosing, whereas ≥90% receptor occupancy was achieved by Day 3 and was consistently maintained in all tissues with SC QW dosing. As a result of this difference, the 120 mg SC QW dosing was selected as the dosage for planned phase III trials in patients with other diseases (e.g., systemic sclerosis).[14]

This study has certain limitations. First, the impact of disease pathology, age, and race on IFNAR1 abundance is not clearly established. It was assumed there is no clinically relevant impact of these covariates on IFNAR1 expression. IFNAR1 receptor expression was optimized by a relative transcriptomics approach and modeling and not by experimental absolute quantification of IFNAR1 abundance in tissues. As the anifrolumab PBPK model adequately predicted the pharmacokinetics over a large dose range, it indirectly validated the receptor expression predicted by the relative transcriptomics approach and can be considered a good representation of in vivo IFNAR1 expression. Comparison of absolute IFNAR1 abundance in clinical studies to the relative transcriptomics estimate provided external validation: absolute serum IFNAR1 abundance ranged from 0 to 0.17 nM (0–25 ng/mL) in clinical studies[37,44] and was estimated to be 0.11 nM using relative transcriptomics (Appendix S1: Section 2.4, Table S8). Meyer et al.[31] used a similar approach

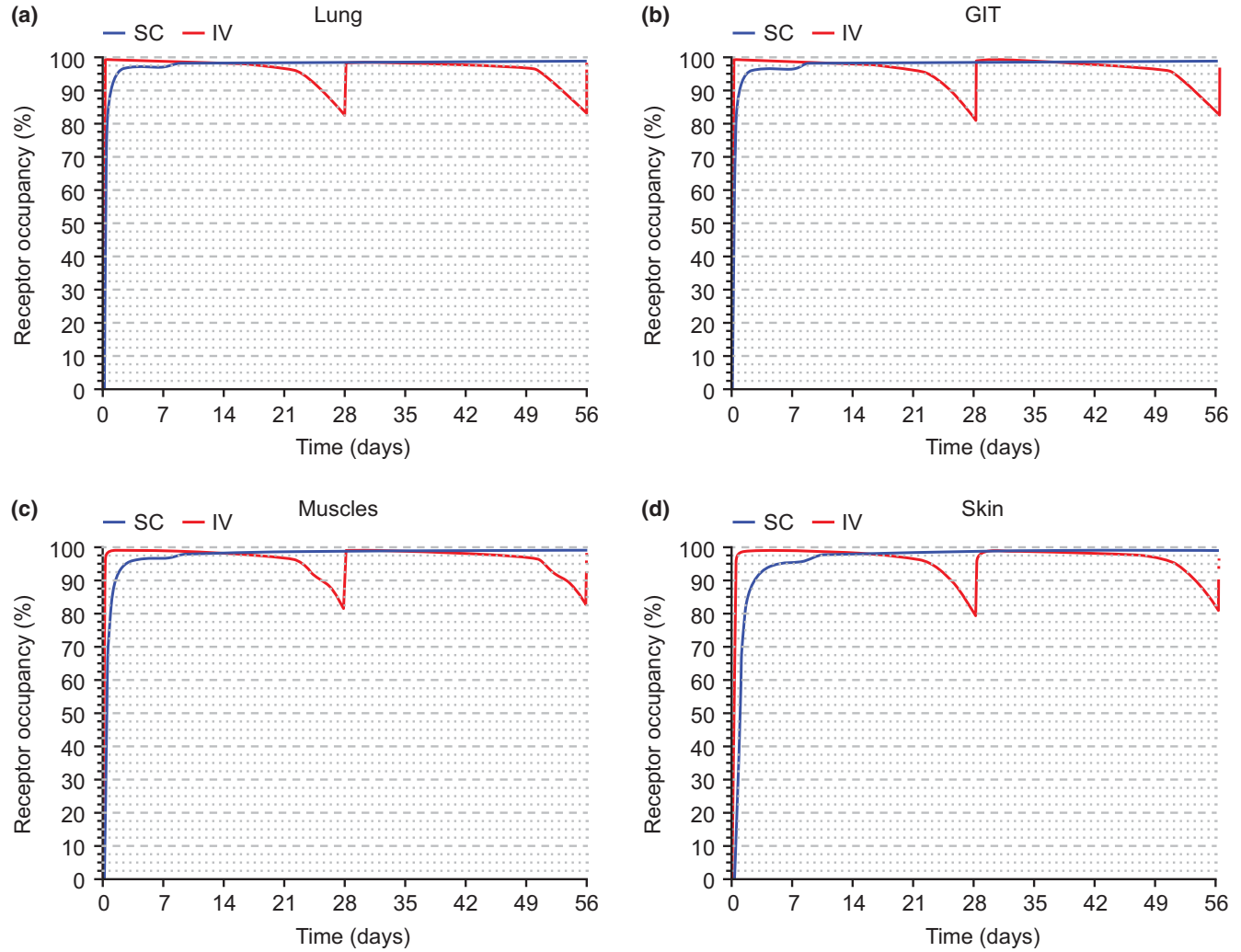

FIGURE 5 Comparison of mean IFNAR1 receptor occupancy (%) of anifrolumab after 300 mg IV Q4W and 120 mg SC QW dosing in the SSc and SLE patient population in (a) lung, (b) GIT, (c) muscles, and (d) skin; the solid red and blue lines represent the predicted mean receptor occupancy (%) after IV and SC dosing, respectively ($n = 100$). GIT, gastrointestinal tract; IFNAR1, type I interferon receptor; IV, intravenous; Q4W, every 4 weeks; QW, once a week; SC, subcutaneous; SLE, systemic lupus erythematosus; SSc, systemic sclerosis.

for drug transporter proteins (OATP1B1, OAT3, and MRP2) to predict the clinical pharmacokinetics of pravastatin. Second, the modeling approach used a built-in structural PBPK model with most parameters fixed based on endogenous IgG behavior. Anifrolumab in vitro values of FcRn K_d, and clinical data were used to parameterize the TMDD aspects of the model and predict the compound pharmacokinetics in a population. Since faster IgG elimination has been reported in patients with SLE,[45] and a study in mouse models with lupus-like autoimmune syndromes reported several-fold increases in IgG clearance,[46] non-specific CL_{cat} was optimized in the anifrolumab PBPK model. Like population pharmacokinetics modeling analysis, our PBPK analysis shows higher catabolic clearance in patients vs. healthy volunteers (0.0175 L/h vs 0.0053 L/h). Although there is no published clinical study quantifying CL_{cat} of IgG in humans, CL_{cat} optimized for patients with autoimmune inflammation vs. healthy patients in our study matches the results of clinical studies for similar IgGs in other inflammatory conditions. For example, Chakraborty et al.[47] reported IV canakinumab clearances of 0.0076 L/h in patients with cryopyrin-associated periodic syndromes (CAPS), 0.0083–0.0118 L/h in patients with rheumatoid arthritis, 0.005–0.0057 L/h in a healthy Caucasian population, and 0.0067–0.0073 L/h in Japanese healthy volunteers. Furthermore, Wang et al.[48] reported IgG antibody mavrilumab CL_{cat} of 0.011 L/h in patients with rheumatoid arthritis.

While the pharmacokinetics–pharmacodynamics and pharmacokinetics–efficacy relationships are established for anifrolumab in patients with SLE,[42,49] there is limited understanding of the relationship between pharmacokinetics, pharmacodynamics, and efficacy with the SC dose in other indications (e.g., SSc, myositis, and cutaneous lupus erythematosus). As such, further work is needed

to establish pharmacokinetics–efficacy relationships in these indications.

We developed the anifrolumab PBPK model utilizing data from preclinical, clinical, and published data. We validated the model over a wide range of clinical scenarios, and uniquely, used a relative transcriptomics approach for predicting IFNAR1 abundance in target tissues. The validated anifrolumab PBPK model predicted high local unbound anifrolumab concentrations in target tissues well over anifrolumab affinity for IFNAR1, resulting in high receptor occupancy with both 300 mg IV Q4W and 120 mg SC QW. The validated model predicted that 120 mg SC QW dosing is likely to provide sustained high receptor occupancy and similar or improved efficacy to the approved 300 mg IV Q4W dosing. These results support proposed dosing and administration recommendations for anifrolumab phase III studies for new indications, including in patients with SSc.

AUTHOR CONTRIBUTIONS

P.S., D.W.B., L.N.B., and W.T. wrote the manuscript; P.S., D.W.B., L.N.B., and W.T. designed the research; P.S., L.N.B., and W.T. performed the research; P.S., L.N.B., and W.T. analyzed the data.

ACKNOWLEDGMENTS

The authors would like to thank the investigators, research staff, health care providers, and especially the patients who participated in the studies that informed the development of this PBPK model. The views expressed in this publication are those of the author(s). Medical writing support was provided by Heather Hultzapple, PharmD, Rosie Butler, PhD, and Vasileios Stamou, PhD, of JK Associates Inc., part of Avalere Health. This support was funded by AstraZeneca.

FUNDING INFORMATION

This study was sponsored by AstraZeneca.

CONFLICT OF INTEREST STATEMENT

P.S., D.W.B., L.N.B., and W.T. are employees of and hold stock in AstraZeneca.

DATA AVAILABILITY STATEMENT

Data underlying the findings described in this manuscript may be obtained in accordance with AstraZeneca's data sharing policy described at https://astrazenecagrouptrials.pharmacm.com/ST/Submission/Disclosure. Reuse is permitted only with permission from AstraZeneca. The model workspaces can be accessed through the Simcyp Members' Area public repository and upon direct request, and subject to review, AstraZeneca will provide the workspaces of this study.

ORCID

Pradeep Sharma https://orcid.org/0000-0003-3415-8917
David W. Boulton https://orcid.org/0000-0002-0668-7304
Lynn N. Bertagnolli https://orcid.org/0000-0002-3992-5620
Weifeng Tang https://orcid.org/0000-0002-8261-8116

REFERENCES

1. Assassi S, Mayes MD, Arnett FC, et al. Systemic sclerosis and lupus: points in an interferon-mediated continuum. *Arthritis Rheum*. 2010;62:589-598.
2. Greenberg SA, Higgs BW, Morehouse C, et al. Relationship between disease activity and type 1 interferon-and other cytokine-inducible gene expression in blood in dermatomyositis and polymyositis. *Genes Immun*. 2012;13:207-213.
3. Kakkar V, Assassi S, Allanore Y, et al. Type 1 interferon activation in systemic sclerosis: a biomarker, a target or the culprit. *Curr Opin Rheumatol*. 2022;34:357-364.
4. Pinal-Fernandez I, Casal-Dominguez M, Derfoul A, et al. Identification of distinctive interferon gene signatures in different types of myositis. *Neurology*. 2019;93:e1193-e1204.
5. Riggs JM, Hanna RN, Rajan B, et al. Characterisation of anifrolumab, a fully human anti-interferon receptor antagonist antibody for the treatment of systemic lupus erythematosus. *Lupus Sci Med*. 2018;5:e000261.
6. Saphnelo Prescribing Information. https://den8dhaj6zs0e.cloudfront.net/50fd68b9-106b-4550-b5d0-12b045f8b184/44b6985c-8268-46b1-ba3e-2bb43bfd4d4c/44b6985c-8268-46b1-ba3e-2bb43bfd4d4c_viewable_rendition__v.pdf. Accessed 15 Sep 2023.
7. Fanouriakis A, Kostopoulou M, Andersen J, et al. EULAR recommendations for the management of systemic lupus erythematosus: 2023 update. *Ann Rheum Dis*. 2023;83:15-29.
8. Pope JE, Denton CP, Johnson SR, Fernandez-Codina A, Hudson M, Nevskaya T. State-of-the-art evidence in the treatment of systemic sclerosis. *Nat Rev Rheumatol*. 2023;19:212-226.
9. Furie R, Khamashta M, Merrill JT, et al. Anifrolumab, an anti-interferon-α receptor monoclonal antibody, in moderate-to-severe systemic lupus erythematosus. *Arthritis Rheumatol*. 2017;69:376-386.
10. Furie RA, Morand EF, Bruce IN, et al. Type I interferon inhibitor anifrolumab in active systemic lupus erythematosus (TULIP-1): a randomised, controlled, phase 3 trial. *Lancet Rheumatol*. 2019;1:e208-e219.
11. Morand EF, Furie R, Tanaka Y, et al. Trial of Anifrolumab in active systemic lupus erythematosus. *N Engl J Med*. 2020;382:211-221.
12. Chia YL, Santiago L, Wang B, et al. Exposure-response analysis for selection of optimal dosage regimen of anifrolumab in patients with systemic lupus erythematosus. *Rheumatology (Oxford)*. 2021;60:5854-5862.
13. Almquist J, Kuruvilla D, Mai T, et al. Nonlinear population pharmacokinetics of Anifrolumab in healthy volunteers and patients with systemic lupus erythematosus. *J Clin Pharmacol*. 2022;62:1106-1120.
14. ClinicalTrials.gov. Determine effectiveness of anifrolumab in systemic sclerosis (DAISY). https://clinicaltrials.gov/study/NCT05925803. Accessed 15 Sep 2023.

15. ClinicalTrials.gov. A study to investigate the efficacy and safety of anifrolumab in adults with chronic and/or subacute cutaneous lupus erythematosus (LAVENDER). https://classic.clinicaltrials.gov/ct2/show/NCT06015737. Accessed 28 Nov 2023.
16. AstraZeneca. A study to investigate the efficacy and safety of anifrolumab administered as subcutaneous injection and added to standard of care compared with placebo added to standard of care in adult participants with polymyositis (JASMINE). https://www.astrazenecaclinicaltrials.com/study/D3463C00003/. Accessed 28 Nov 2023.
17. ClinicalTrials.gov. Subcutaneous anifrolumab in adult patients with systemic lupus erythematosus (Tulip SC). https://clinicaltrials.gov/study/NCT04877691. Accessed 29 Nov 2023.
18. Tummala R, Rouse T, Berglind A, Santiago L. Safety, tolerability and pharmacokinetics of subcutaneous and intravenous anifrolumab in healthy volunteers. *Lupus Sci Med*. 2018;5:e000252.
19. Dashiell-Aje E, Harding G, Pascoe K, DeVries J, Berry P, Ramachandran S. Patient evaluation of satisfaction and outcomes with an autoinjector for self-Administration of Subcutaneous Belimumab in patients with systemic lupus erythematosus. *Patient*. 2018;11:119-129.
20. Falanga M, Canzona A, Mazzoni D. Preference for subcutaneous injection or intravenous infusion of biological therapy among Italian patients with SLE. *J Patient Exp*. 2019;6:41-45.
21. Zhuang X, Lu C. PBPK modeling and simulation in drug research and development. *Acta Pharm Sin B*. 2016;6:430-440.
22. Kalra P, Brandl J, Gaub T, et al. Quantitative systems pharmacology of interferon alpha administration: a multi-scale approach. *PLoS One*. 2019;14:e0209587.
23. ClinicalTrials.gov. Phase 3 Study of Anifrolumab in Adult Patients With Active Proliferative Lupus Nephritis (IRIS). https://www.clinicaltrials.gov/study/NCT05138133. Accessed 28 Nov 2023.
24. Goldberg A, Geppert T, Schiopu E, et al. Dose-escalation of human anti-interferon-α receptor monoclonal antibody MEDI-546 in subjects with systemic sclerosis: a phase 1, multicenter, open label study. *Arthritis Res Ther*. 2014;16:R57.
25. Tanaka Y, Takeuchi T, Okada M, et al. Safety and tolerability of anifrolumab, a monoclonal antibody targeting type I interferon receptor, in Japanese patients with systemic lupus erythematosus: a multicenter, phase 2, open-label study. *Mod Rheumatol*. 2020;30:101-108.
26. Jamei M, Marciniak S, Feng K, Barnett A, Tucker G, Rostami-Hodjegan A. The Simcyp population-based ADME simulator. *Expert Opin Drug Metab Toxicol*. 2009;5:211-223.
27. Chetty M, Li L, Rose R, et al. Prediction of the pharmacokinetics, pharmacodynamics, and efficacy of a monoclonal antibody, using a physiologically based pharmacokinetic FcRn model. *Front Immunol*. 2014;5:670.
28. Li L, Gardner I, Dostalek M, Jamei M. Simulation of monoclonal antibody pharmacokinetics in humans using a minimal physiologically based model. *AAPS J*. 2014;16:1097-1109.
29. Gill KL, Gardner I, Li L, Jamei M. A bottom-up whole-body physiologically based pharmacokinetic model to mechanistically predict tissue distribution and the rate of subcutaneous absorption of therapeutic proteins. *AAPS J*. 2016;18:156-170.
30. Wong H, Chow TW. Physiologically based pharmacokinetic modeling of therapeutic proteins. *J Pharm Sci*. 2017;106:2270-2275.
31. Meyer M, Schneckener S, Ludewig B, Kuepfer L, Lippert J. Using expression data for quantification of active processes in physiologically based pharmacokinetic modeling. *Drug Metab Dispos*. 2012;40:892-901.
32. The Human Protein Atlas. https://www.proteinatlas.org/ENSG00000142166-IFNAR1/tissue. Accessed 14 Sept 2023.
33. Uhlén M, Fagerberg L, Hallström BM, et al. Proteomics. Tissue-based map of the human proteome. *Science*. 2015;347:1260419.
34. Chandra PK, Gunduz F, Hazari S, et al. Impaired expression of type I and type II interferon receptors in HCV-associated chronic liver disease and liver cirrhosis. *PLoS One*. 2014;9:e108616.
35. Yang L, Zhang X, Huang X, et al. Correlation between IFNAR1 expression in peripheral blood T lymphocytes and inflammatory cytokines, tumor-infiltrating lymphocytes, and chemosensitivity in patients with colorectal cancer. *Cytokine*. 2022;159:156008.
36. Gui J, Gober M, Yang X, et al. Therapeutic elimination of the type 1 interferon receptor for treating psoriatic skin inflammation. *J Invest Dermatol*. 2016;136:1990-2002.
37. Ambrus JL Sr, Dembinski W, Ambrus JL Jr, et al. Free interferon-alpha/beta receptors in the circulation of patients with adenocarcinoma. *Cancer*. 2003;98:2730-2733.
38. Gibiansky L, Gibiansky E, Kakkar T, Ma P. Approximations of the target-mediated drug disposition model and identifiability of model parameters. *J Pharmacokinet Pharmacodyn*. 2008;35:573-591.
39. Shi H, Gudjonsson JE, Kahlenberg JM. Treatment of cutaneous lupus erythematosus: current approaches and future strategies. *Curr Opin Rheumatol*. 2020;32:208-214.
40. Crow MK, Ronnblom L. Type I interferons in host defence and inflammatory diseases. *Lupus Sci Med*. 2019;6:e000336.
41. de Weerd NA, Nguyen T. The interferons and their receptors–distribution and regulation. *Immunol Cell Biol*. 2012;90:483-491.
42. Chia YL, Tummala R, Mai TH, et al. Relationship between Anifrolumab pharmacokinetics, pharmacodynamics, and efficacy in patients with moderate to severe systemic lupus erythematosus. *J Clin Pharmacol*. 2022;62:1094-1105.
43. Higgs BW, Liu Z, White B, et al. Patients with systemic lupus erythematosus, myositis, rheumatoid arthritis and scleroderma share activation of a common type I interferon pathway. *Ann Rheum Dis*. 2011;70:2029-2036.
44. Yaugel-Novoa M, Bourlet T, Longet S, Botelho-Nevers E, Paul S. Association of IFNAR1 and IFNAR2 with COVID-19 severity. *Lancet Microbe*. 2023;4:e487.
45. Wochner RD. Hypercatabolism of normal IgG; an unexplained immunoglobulin abnormality in the connective tissue diseases. *J Clin Invest*. 1970;49:454-464.
46. Zhou J, Pop LM, Ghetie V. Hypercatabolism of IgG in mice with lupus-like syndrome. *Lupus*. 2005;14:458-466.
47. Chakraborty A, Tannenbaum S, Rordorf C, et al. Pharmacokinetic and pharmacodynamic properties of canakinumab, a human anti-interleukin-1beta monoclonal antibody. *Clin Pharmacokinet*. 2012;51:e1-e18.
48. Wang B, Lau YY, Liang M, et al. Mechanistic modeling of antigen sink effect for mavrilimumab following intravenous

administration in patients with rheumatoid arthritis. *J Clin Pharmacol*. 2012;52:1150-1161.
49. Chia YL, Zhang J, Tummala R, Rouse T, Furie RA, Morand EF. Relationship of anifrolumab pharmacokinetics with efficacy and safety in patients with systemic lupus erythematosus. *Rheumatology (Oxford)*. 2022;61:1900-1910.

SUPPORTING INFORMATION

Additional supporting information can be found online in the Supporting Information section at the end of this article.

How to cite this article: Sharma P, Boulton DW, Bertagnolli LN, Tang W. Physiology-based pharmacokinetic model with relative transcriptomics to evaluate tissue distribution and receptor occupancy of anifrolumab. *CPT Pharmacometrics Syst Pharmacol*. 2025;14:105-117. doi:10.1002/psp4.13245